Supporting Information

Alkaline-Earth Metal Bis[bis(trimethylsilyl)amide] Complexes with Weakly Coordinating 2,2,5,5-Tetramethyltetrahydrofuran Ligands

Sven Krieck, Philipp Schüler, Helmar Görls, and Matthias Westerhausen

Institute of Inorganic and Analytical Chemistry, Friedrich-Schiller-University Jena
Humboldtstraße 8, D-07743 Jena, Germany
E-mail: m.we@uni-jena.de

Content:

Dissociation equilibria

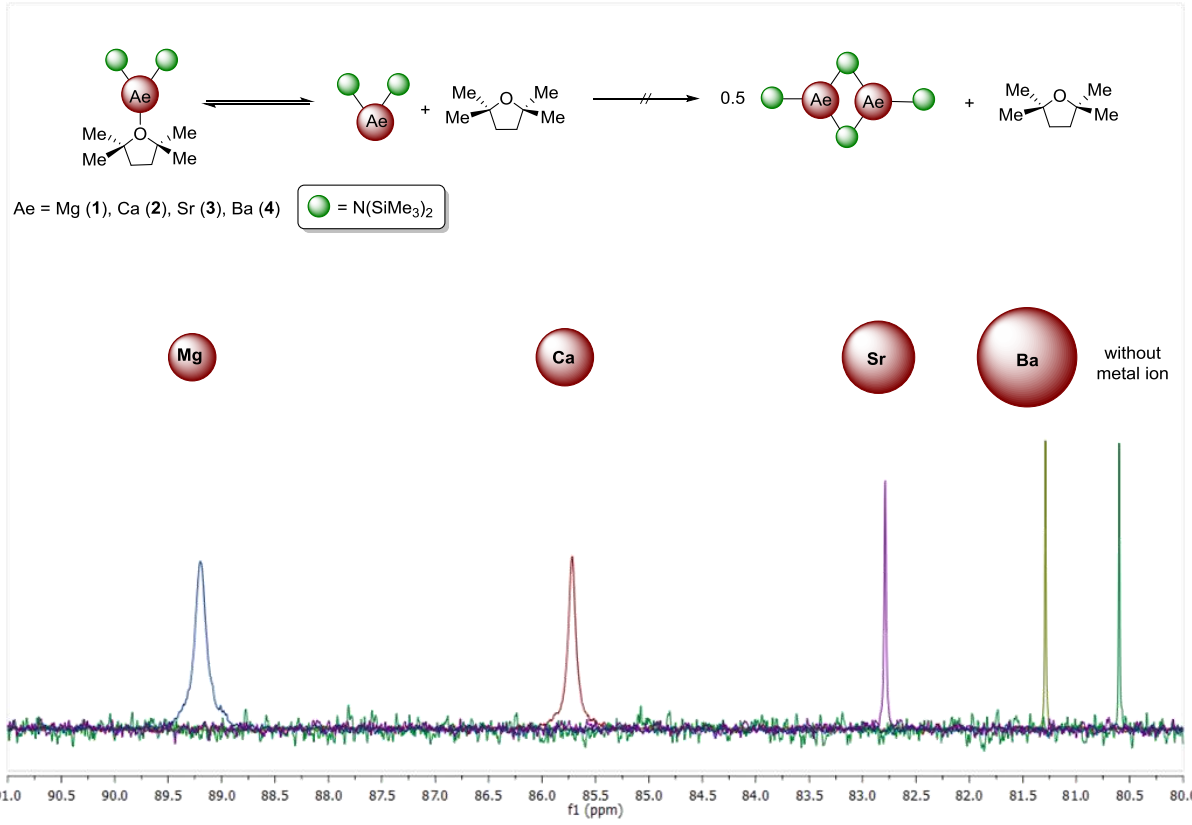

Figure S1: $^{13}C\{^{1}H\}$ NMR signals of quaternary carbon atom of Me_4thf (400 MHz, C_6D_6, 296 K) from the adducts $[(Me_4thf)Ae(hmds)_2]$ (Ae = Mg – Ba).

I. Analytical data

[(Me$_4$thf)Mg(hmds)$_2$] (**1**)

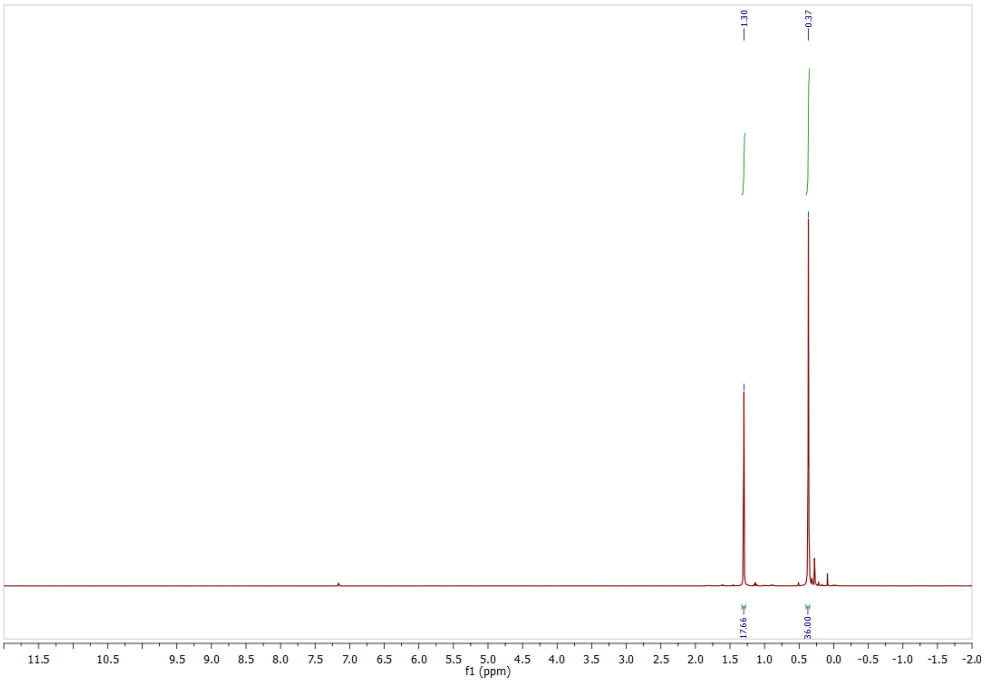

Figure S2: ^{1}H-NMR (400 MHz, C_6D_6, 297 K) of dissolved crystals of [(Me$_4$thf)Mg(hmds)$_2$] **1**.

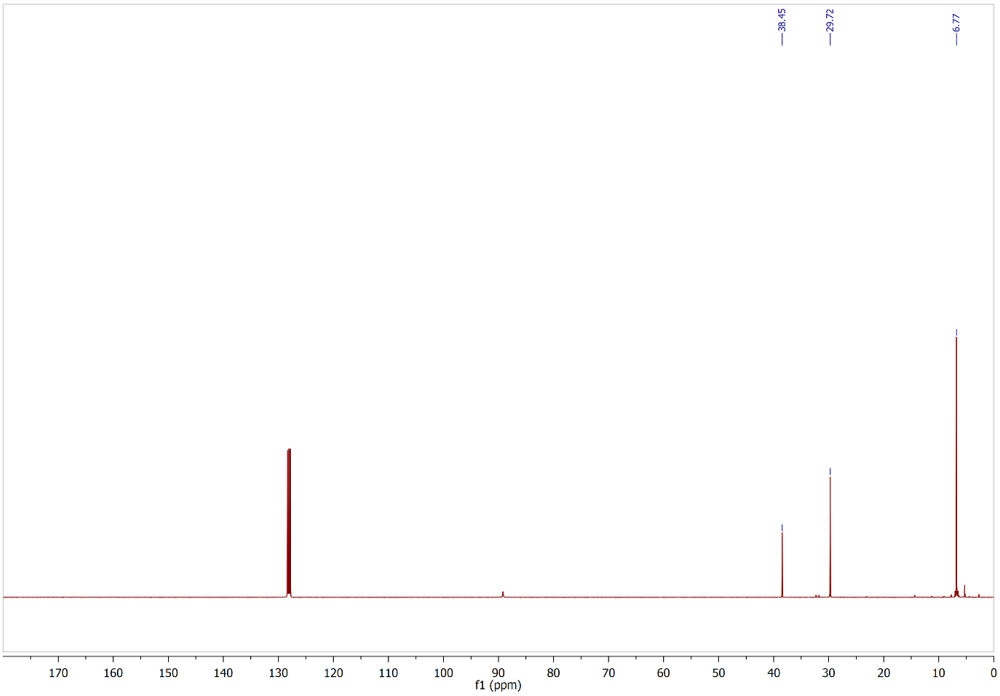

Figure S3: ^{13}C{^{1}H}-NMR (101 MHz, C_6D_6, 297 K) of dissolved crystals of [(Me$_4$thf)Mg(hmds)$_2$] **1**.

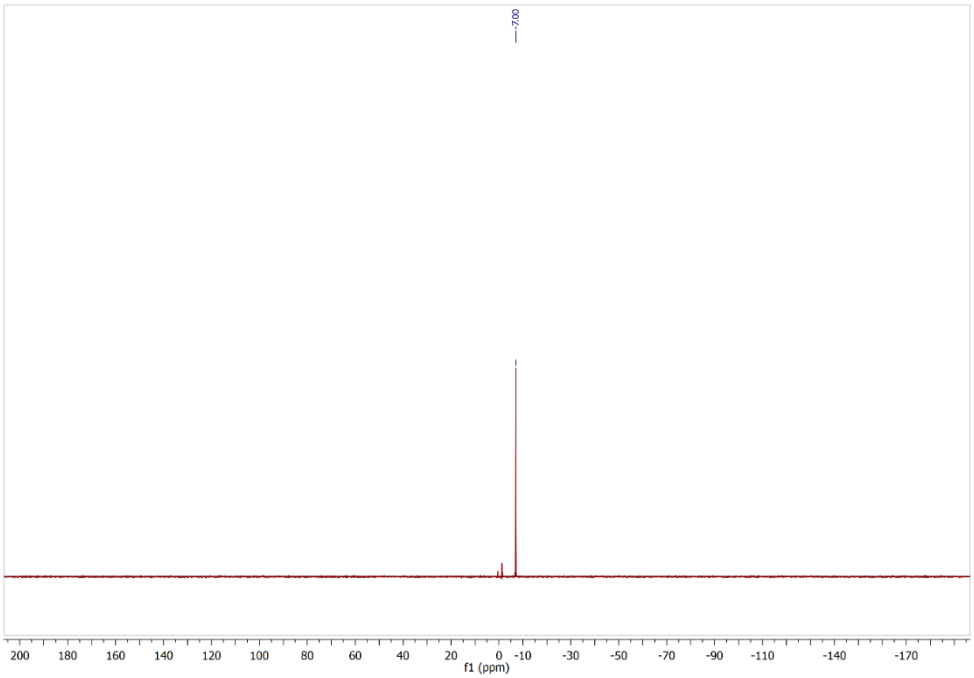

Figure S4: ^{29}Si-^{1}H-DEPT-NMR (79,5 MHz, C_6D_6, 297 K) of dissolved crystals of [$(Me_4thf)Mg(hmds)_2$] **1**.

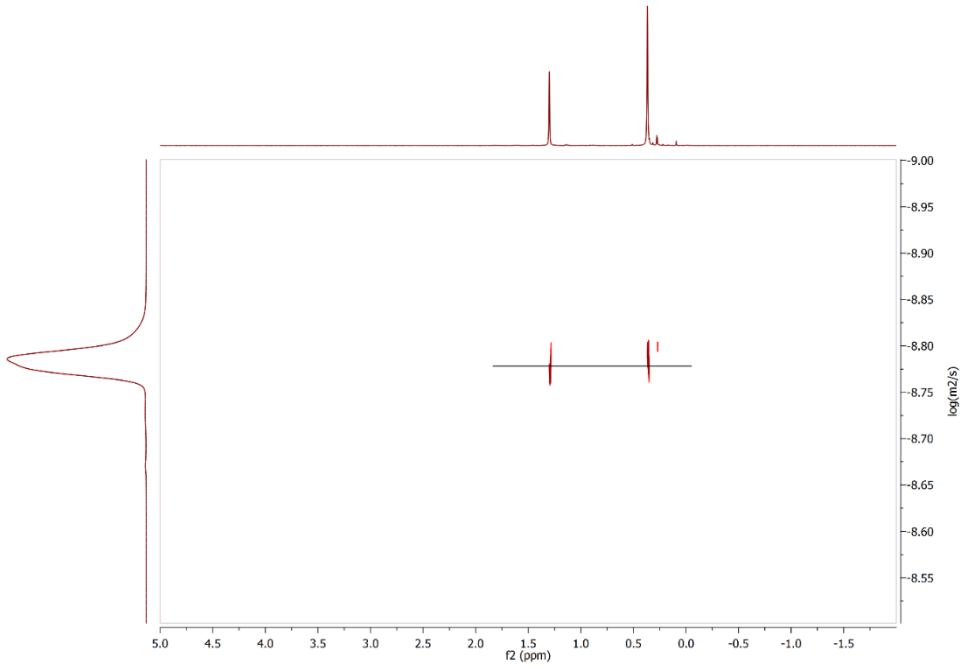

Figure S5: ^{1}H-DOSY (400 MHz, C_6D_6, 297 K) of dissolved crystals of [$(Me_4thf)Mg(hmds)_2$] **1**.

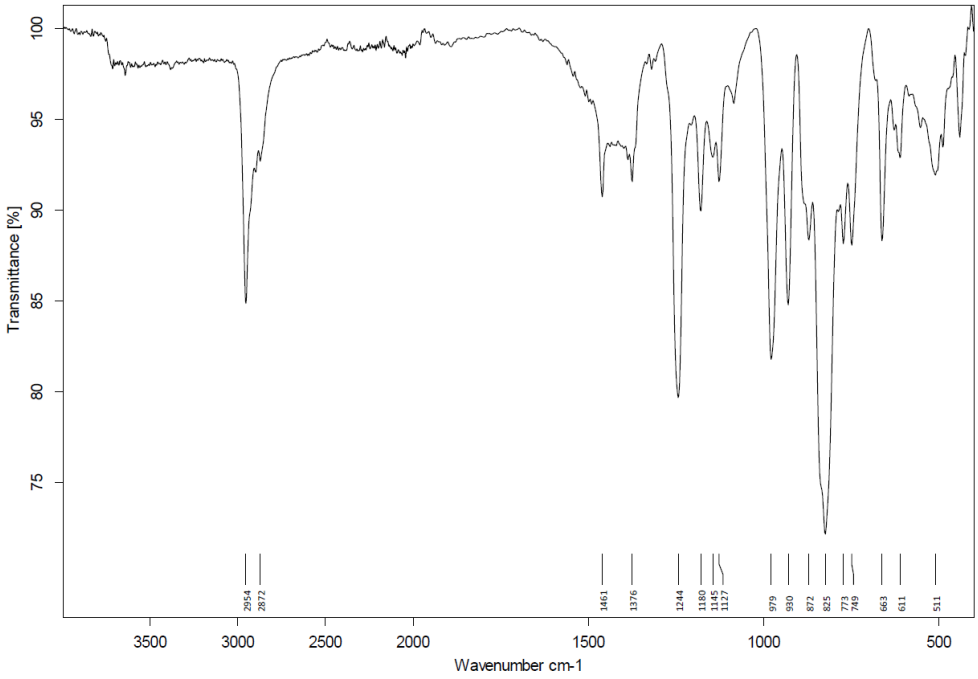

Figure S6: IR (ATR) of [$(Me_4thf)Mg(hmds)_2$] **1**.

[(Me$_4$thf)Ca(hmds)$_2$] (**2**)

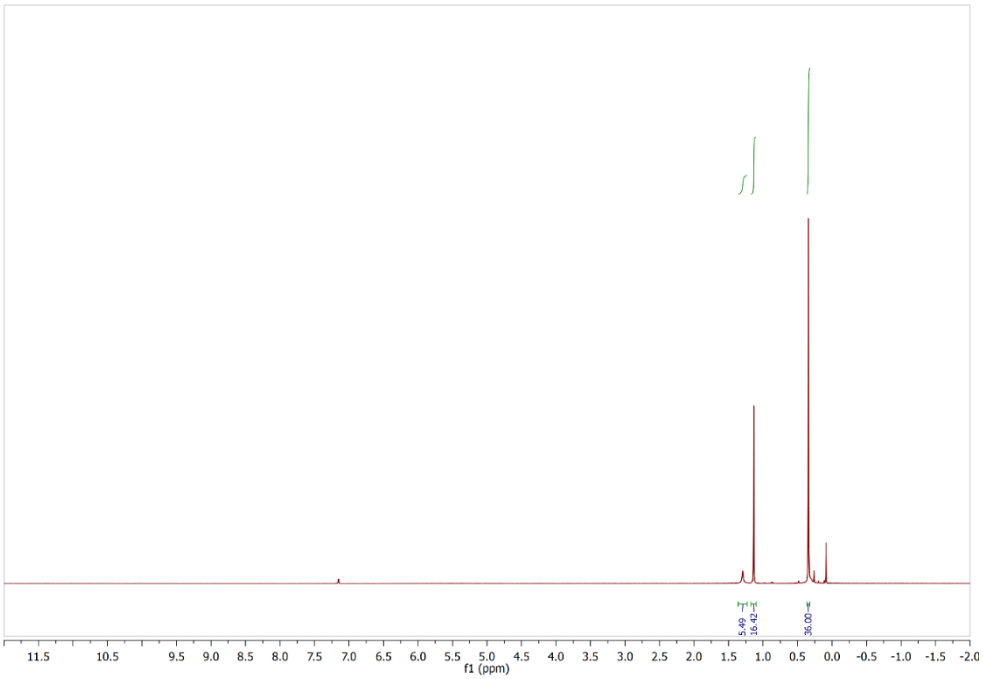

Figure S7: ^{1}H-NMR (400 MHz, C_6D_6, 297K) of dissolved crystals of [(Me$_4$thf)Ca(hmds)$_2$] **2**.

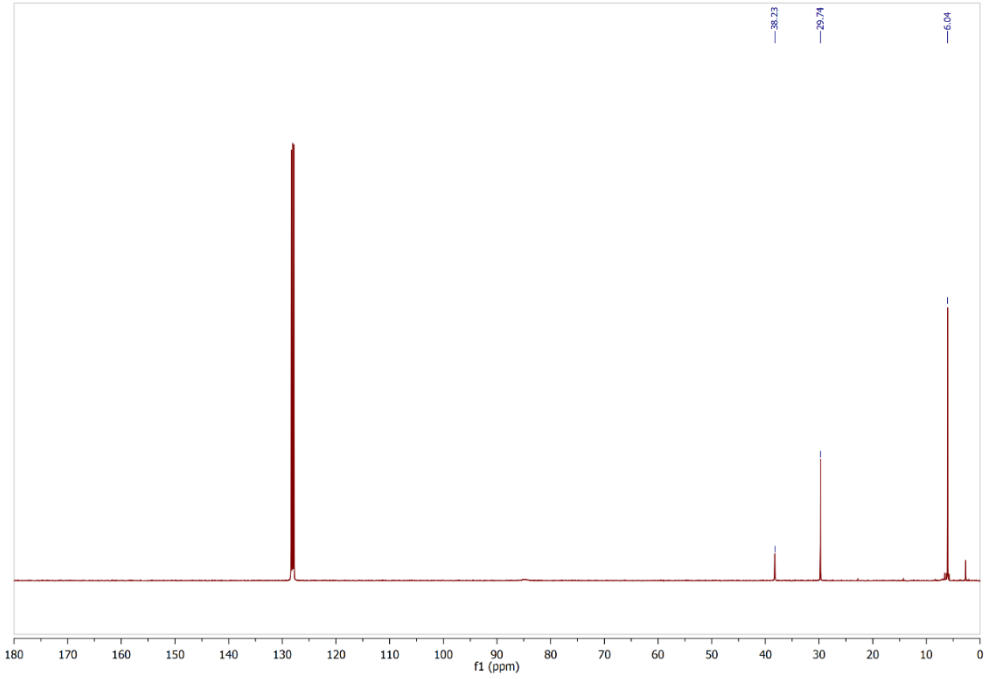

Figure S8: ^{13}C{^{1}H}-NMR (101 MHz, C_6D_6, 297K) of dissolved crystals of [(Me$_4$thf)Ca(hmds)$_2$] **2**.

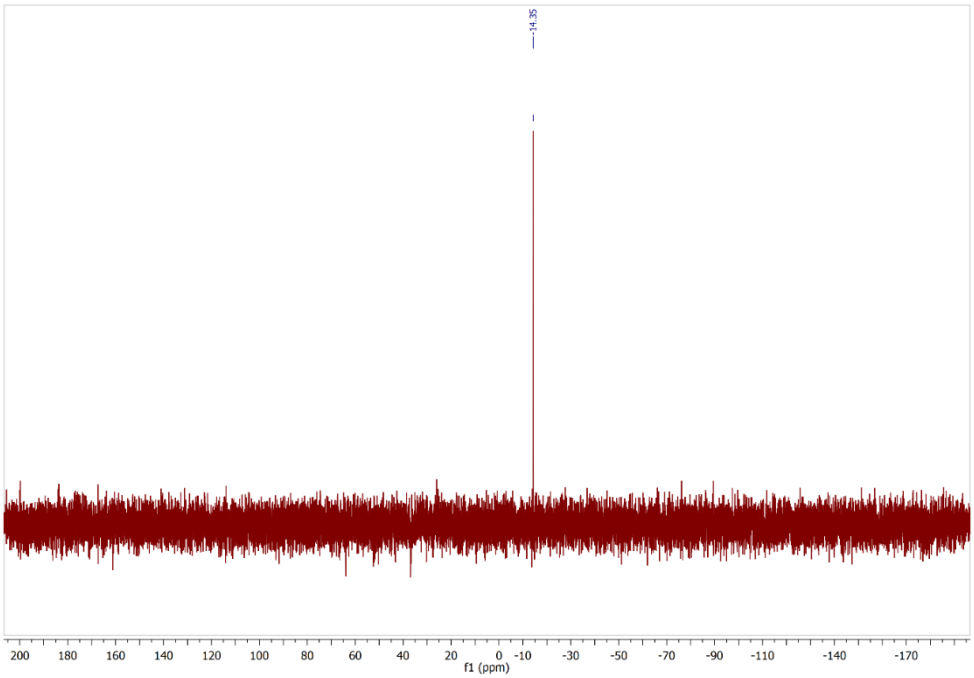

Figure S9: ^{29}Si-^{1}H-DEPT- NMR (79 MHz, C_6D_6, 297K) of dissolved crystals of [$(Me_4thf)Ca(hmds)_2$] **2**.

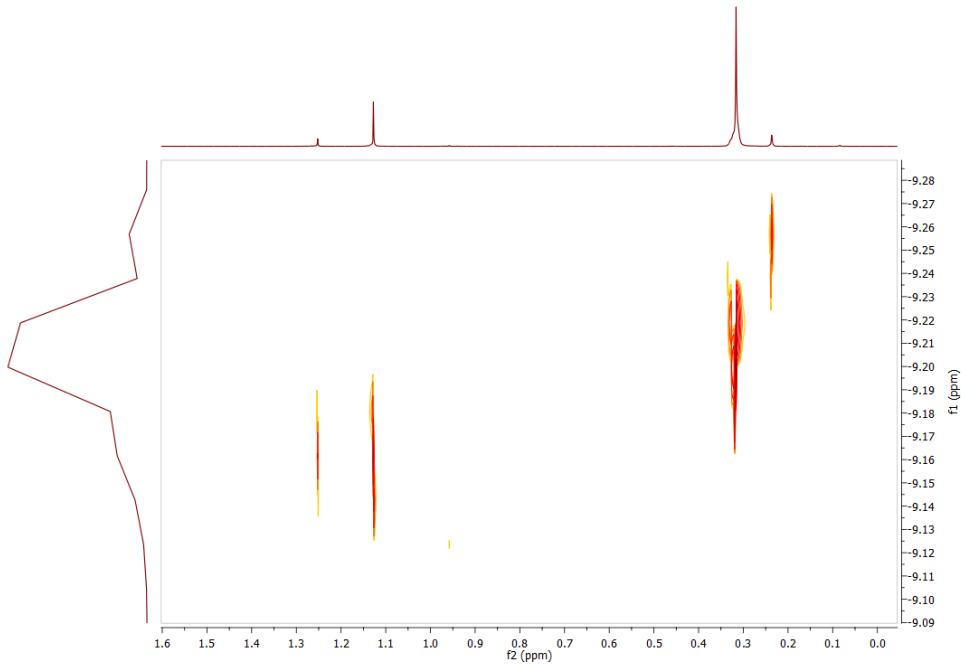

Figure S10: ^{1}H-DOSY-NMR (400 MHz, C_6D_6, 297 K) of dissolved crystals of [$(Me_4thf)Ca(hmds)_2$] **2**.

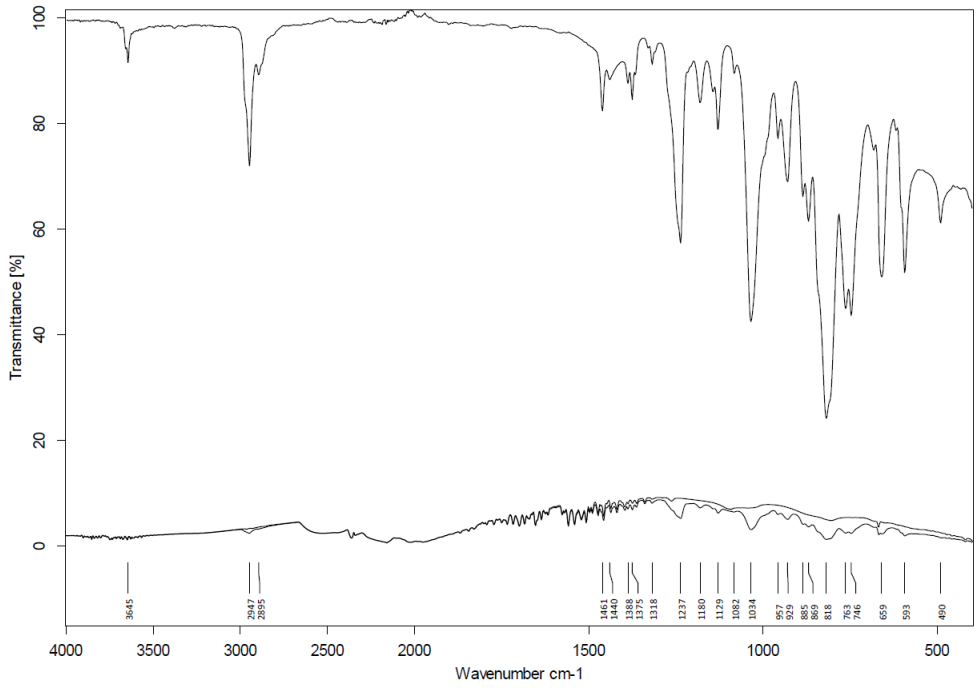

Figure S11: IR (ATR) of [$(Me_4thf)Ca(hmds)_2$] **2**.

[(Me$_4$thf)Sr(hmds)$_2$] (**3**)

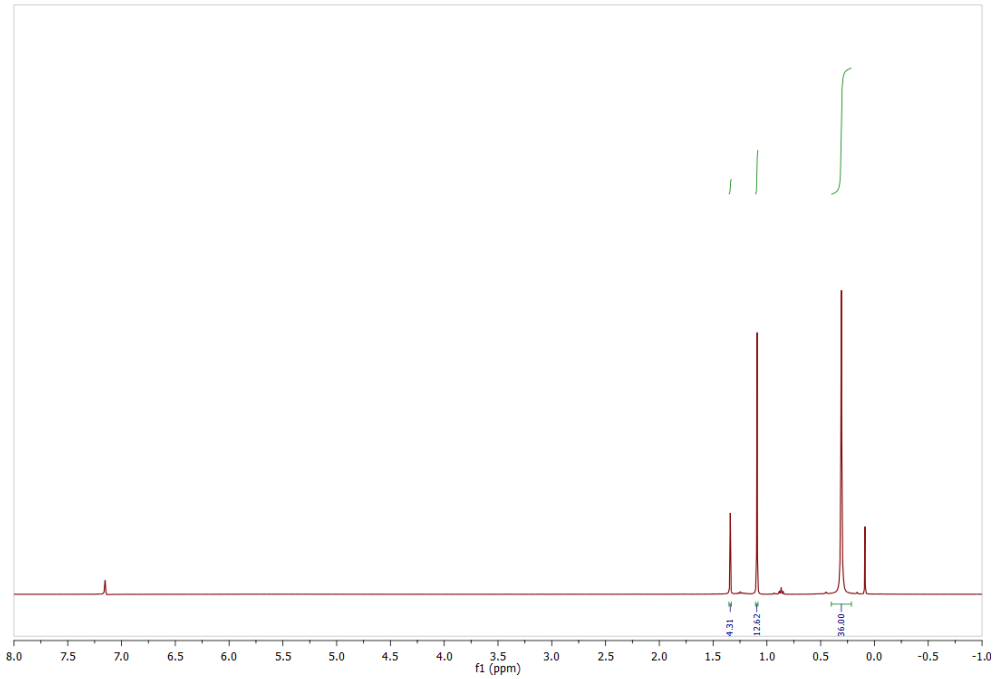

Figure S12: ^{1}H-NMR (400 MHz, C_6D_6. 297 K) of dissolved crystals of [(Me$_4$thf)Sr(hmds)$_2$] **3**.

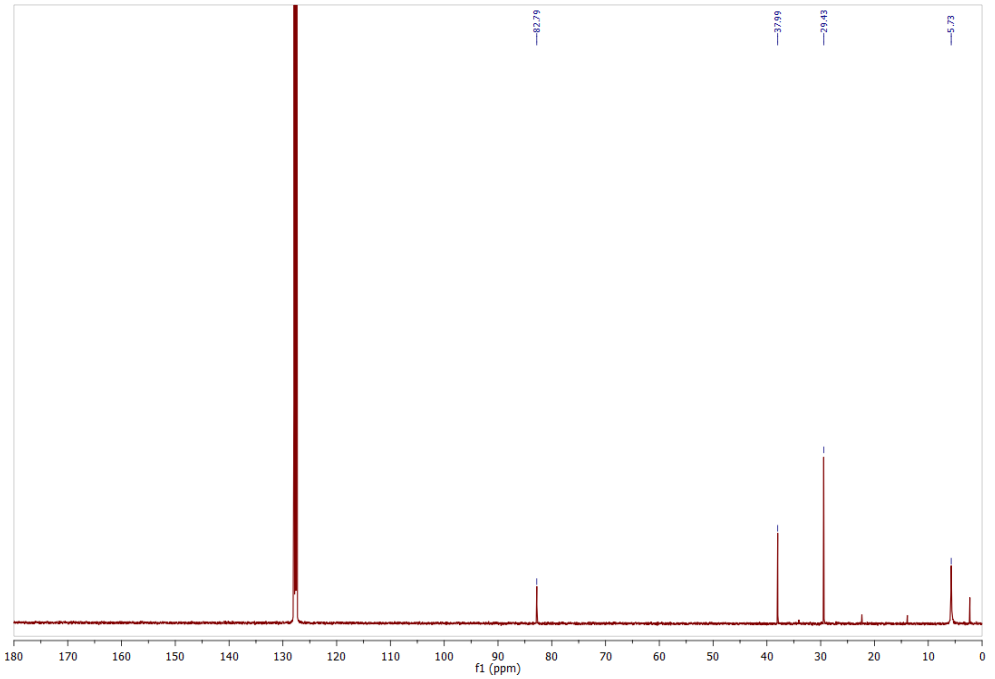

Figure S13: ^{13}C{^{1}H}-NMR (101 MHz, C_6D_6. 297 K) of dissolved crystals of [(Me$_4$thf)Sr(hmds)$_2$] **3**.

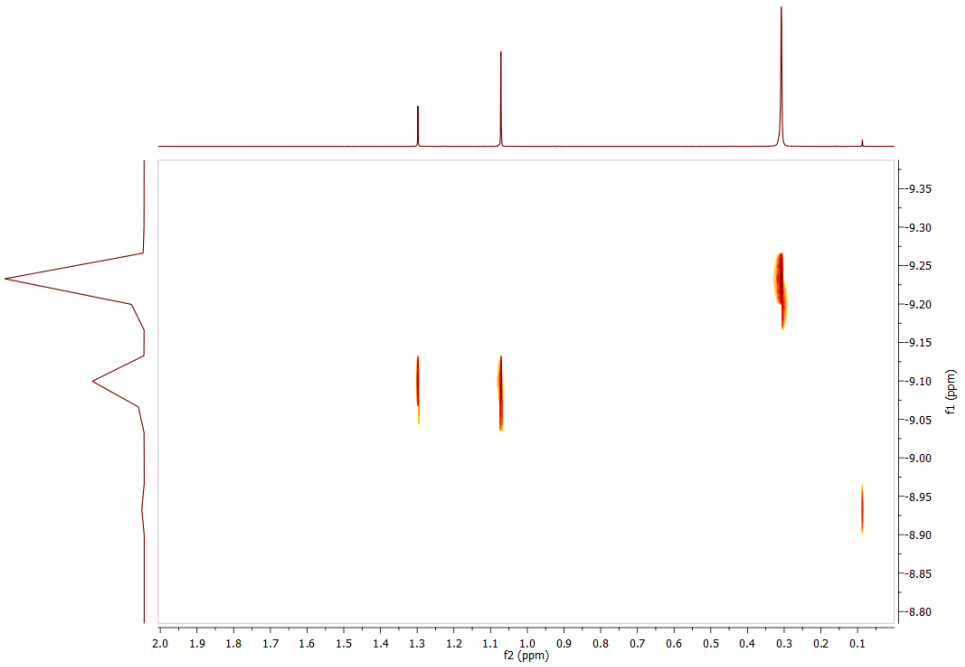

Figure S14: ^{1}H-DOSY-NMR (400 MHz, C_6D_6. 297 K) of dissolved crystals of [$(Me_4thf)Sr(hmds)_2$] **3**.

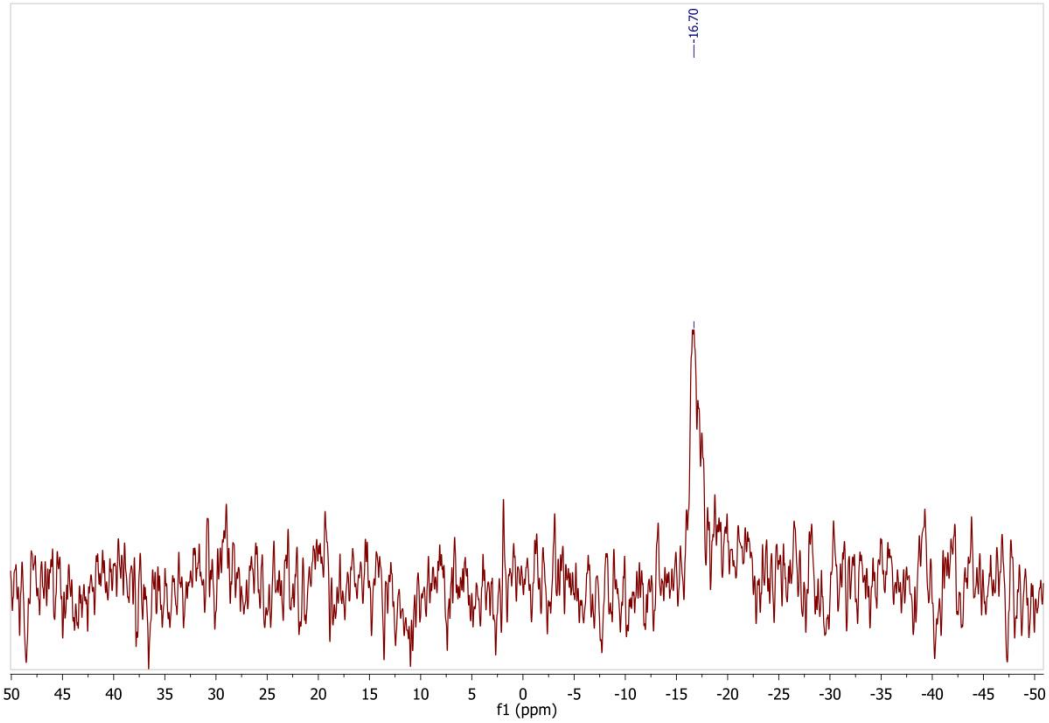

Figure S15: ^{29}Si{^{1}H}-NMR (79.5 MHz, C_6D_6, 296 K) of [$(Me_4thf)Sr(hmds)_2$].

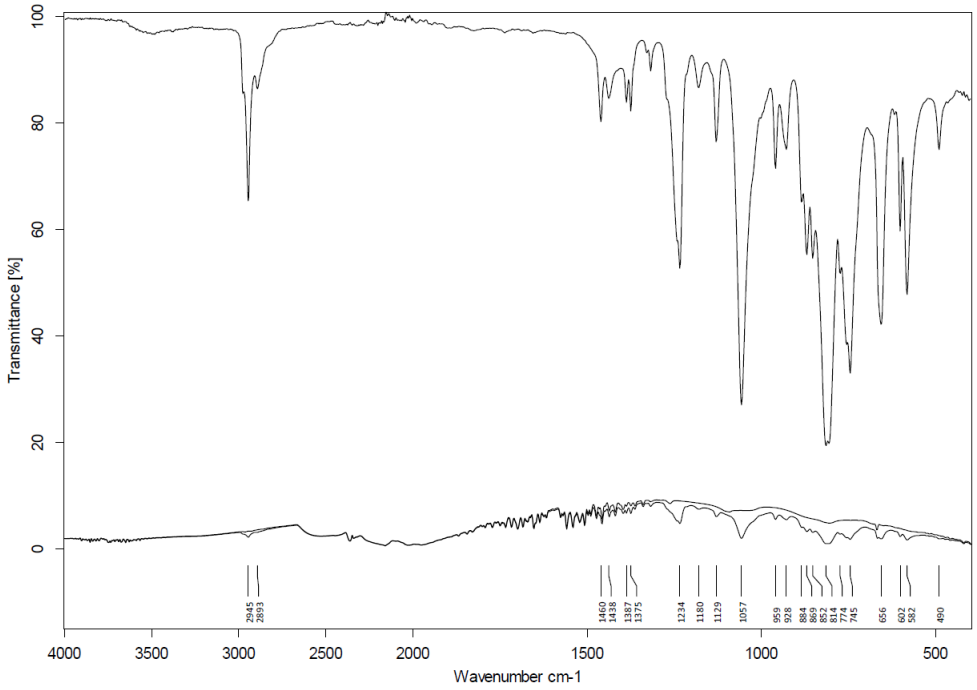

Figure S15: IR (ATR) of [(Me_4thf)Sr(hmds)$_2$] **3**.

[(Me$_4$thf)Ba(hmds)$_2$] (**4**)

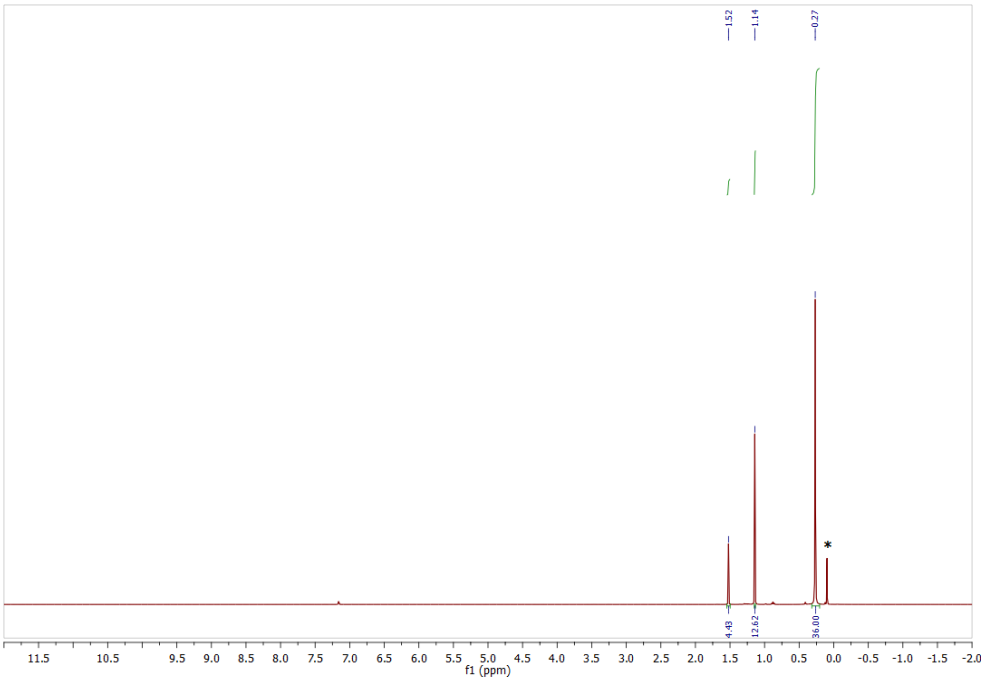

Figure S16: ^{1}H-NMR (400 MHz, C_6D_6, 297 K) of dissolved crystals of [(Me$_4$thf)Ba(hmds)$_2$] **4** (*- H(hmds)).

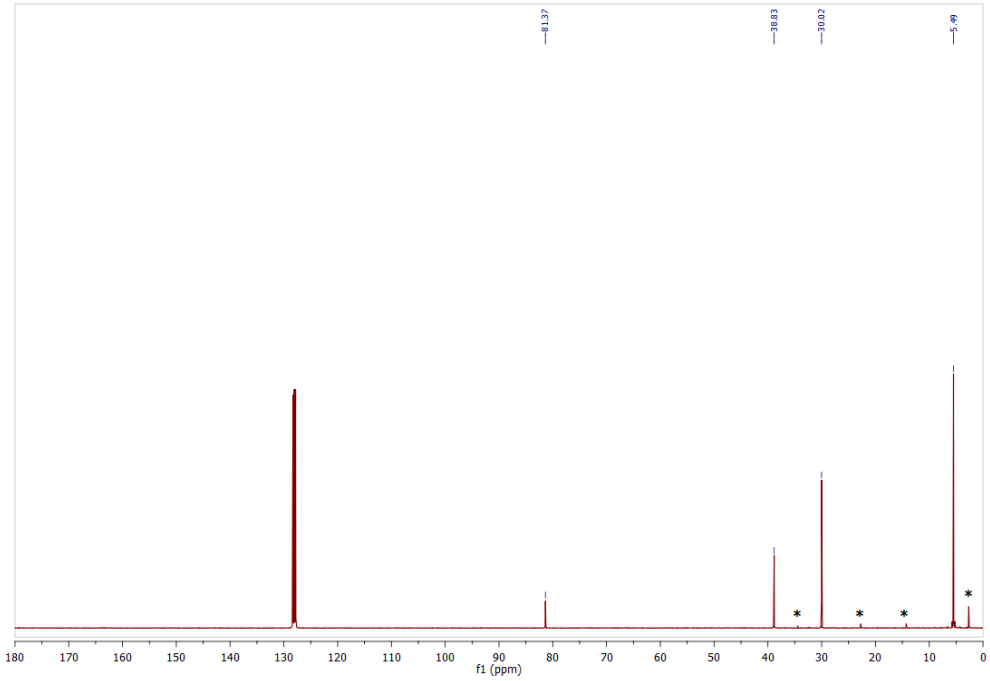

Figure S17: ^{13}C{^{1}H} -NMR (101 MHz, C_6D_6, 297 K) of dissolved crystals of [(Me$_4$thf)Ba(hmds)$_2$] **4** (*-*n*-hexane, H(hmds)).

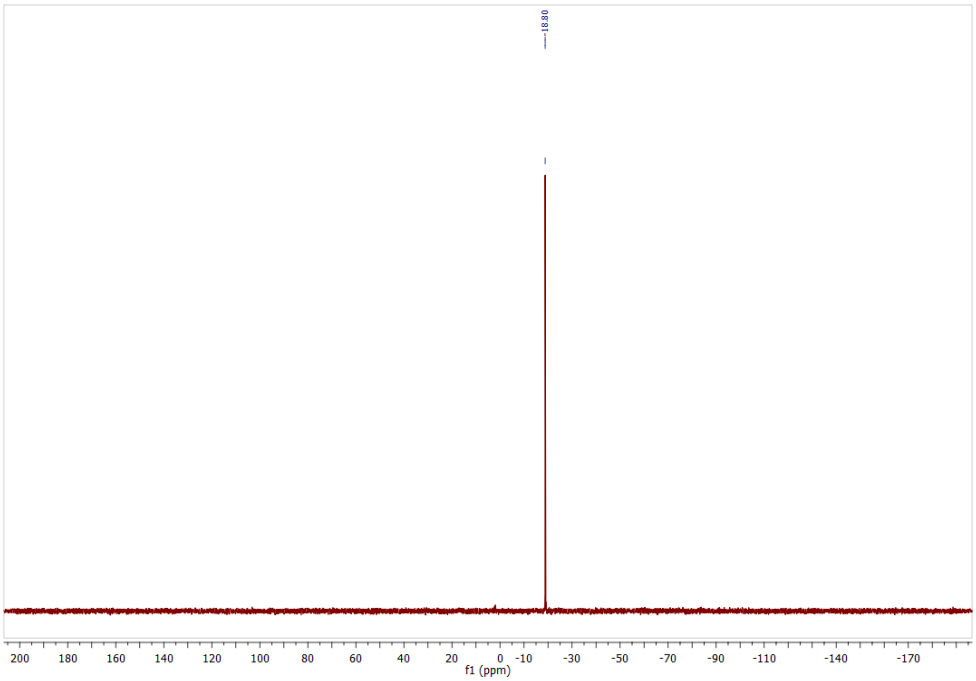

Figure S18: ^{29}Si-^{1}H-DEPT (79,5 MHz, C_6D_6, 297 K) of dissolved crystals of [(Me_4thf)Ba(hmds)$_2$] **4.**

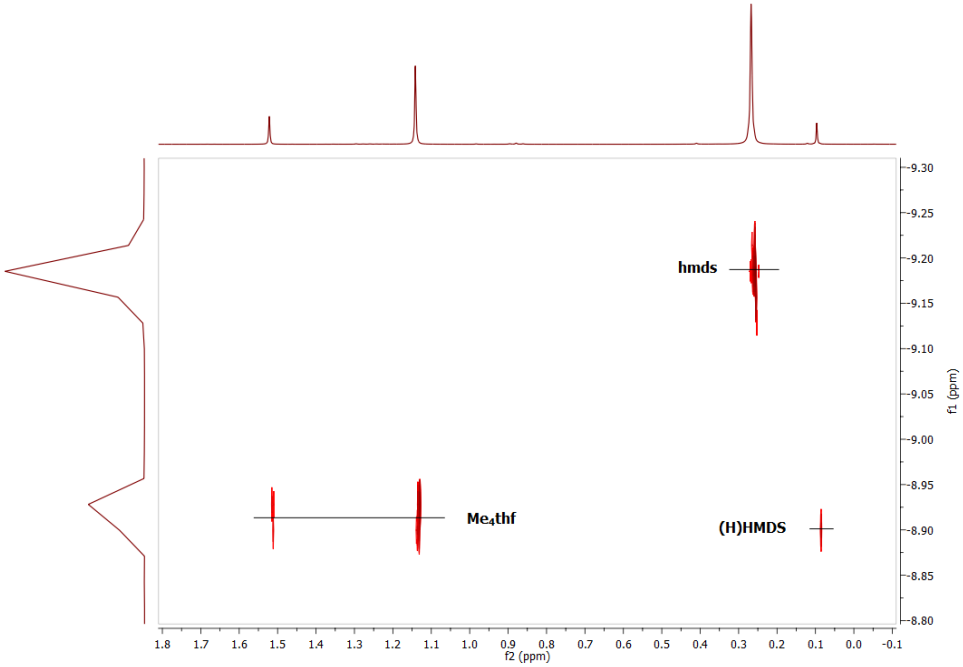

Figure S20: ^{1}H-DOSY (400 MHz, C_6D_6, 297 K) of dissolved crystals of [(Me_4thf)Ba(hmds)$_2$] **4**.

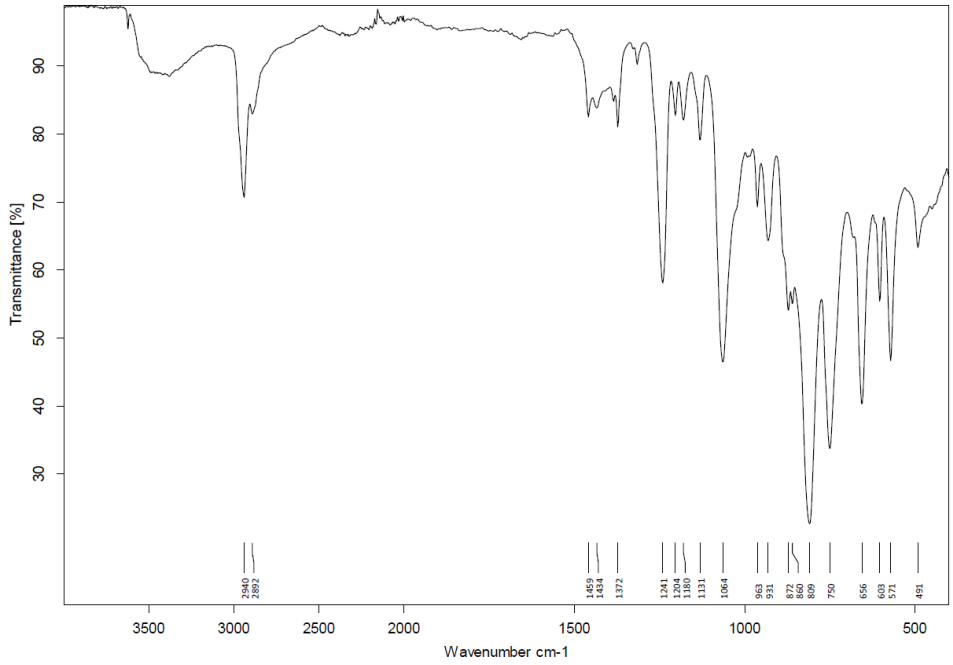

Figure S19: IR (ATR) of [(Me_4thf)Ba(hmds)$_2$] **4**.

Table S1: Crystal data and refinement details for the X-ray structure determinations of the compounds **1** - **4**.

Compound	**1**	**2**	**3**	**4**
formula	$C_{20}H_{52}MgN_2OSi_4$	$C_{20}H_{52}CaN_2OSi_4$	$C_{20}H_{52}N_2OSi_4Sr$	$C_{20}H_{52}BaN_2OSi_4$
fw ($g \cdot mol^{-1}$)	473.31	489.08	536.62	586.34
°C	-140(2)	-140(2)	-140(2)	-140(2)
crystal system	monoclinic	orthorhombic	orthorhombic	triclinic
space group	C 2	C 2 2 2_1	C 2 2 2_1	P $\bar{1}$
a/ Å	18.8311(3)	8.2638(1)	8.2667(17)	10.9264(2)
b/ Å	8.4579(1)	19.4277(4)	19.904(4)	11.4118(2)
c/ Å	18.8139(4)	18.9845(4)	18.906(4)	14.4972(2)
α/°	90	90	90	92.695(1)
β/°	92.4940(10)	90	90	93.785(1)
γ/°	90	90	90	115.177(1)
V/Å^3	2993.68(9)	3047.90(10)	3110.8(11)	1626.70(5)
Z	2	4	4	2
ρ ($g \cdot cm^{-3}$)	1.050	1.066	1.146	1.197
μ (cm^{-1})	2.32	3.76	19	13.8
measured data	11820	9510	10782	10842
data with I > 2σ(I)	6573	3378	3390	7210
unique data (R_{int})	6661/0.0248	3504/0.0243	3492/0.0245	7421/0.0129
wR_2 (all data, on F^2)[a)]	0.1205	0.0595	0.0466	0.0450
R_1 ($I > 2\sigma(I)$) [a)]	0.0475	0.0251	0.0214	0.0192
s [b)]	1.220	1.047	1.053	1.086
Res. dens./$e \cdot Å^{-3}$	0.583/-0.308	0.226/-0.149	0.195/-0.331	0.356/-0.302
Flack-parameter	0.08(14)	0.03(3)	0.000(4)	-
absorpt method	multi-scan	multi-scan	multi-scan	multi-scan
absorpt corr $T_{min}/_{max}$	0.6624/0.7456	0.7123/0.7456	0.6456/0.7456	0.6913/0.7456
CCDC No.	1864053	1864054	1864055	1864056

[a)] Definition of the *R* indices: $R_1 = (\Sigma \, || F_o | - | F_c ||) / \Sigma | F_o |$;
$wR_2 = \{\Sigma[w(F_o^2 - F_c^2)^2] / \Sigma[w(F_o^2)^2]\}^{1/2}$ with $w^{-1} = \sigma^2(F_o^2) + (aP)^2 + bP$; $P = [2F_c^2 + \mathrm{Max}(F_o^2)]/3$;
[b)] $s = \{\Sigma[w(F_o^2 - F_c^2)^2] / (N_o - N_p)\}^{1/2}$.

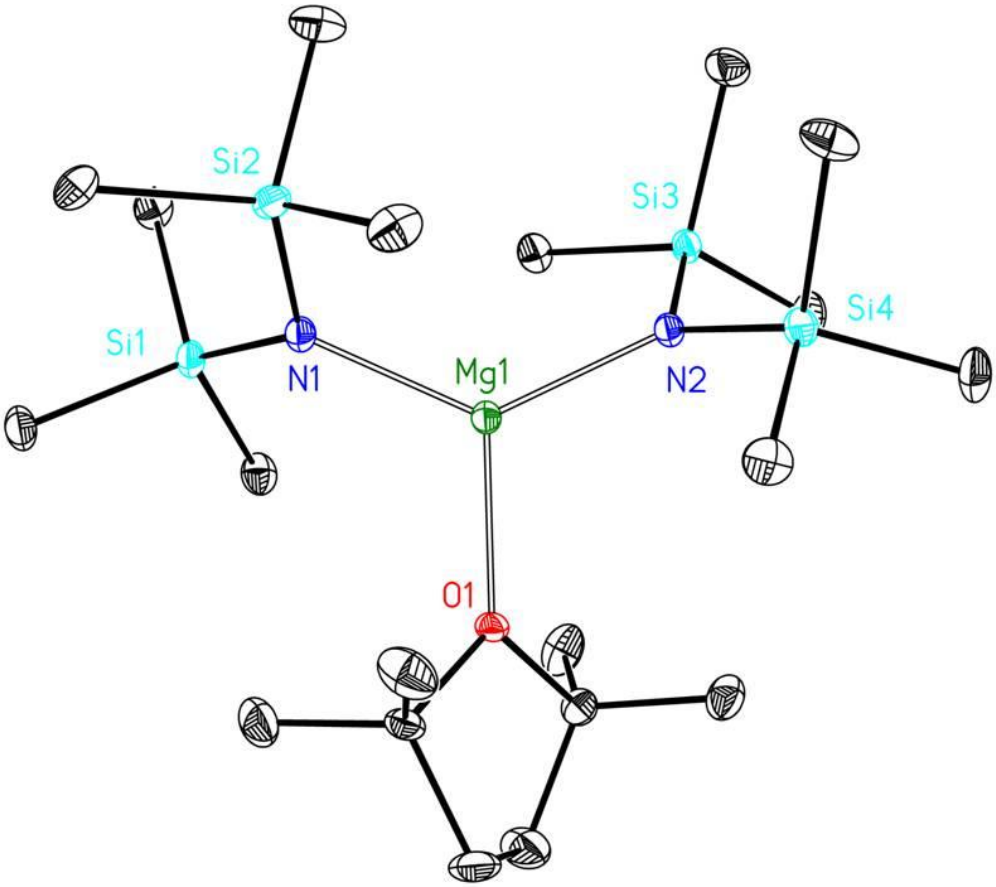

Figure S21: Molecular structure and numbering scheme of $[(Me_4thf)Mg\{N(SiMe_3)_2\}_2]$ (**1**). The ellipsoids represent a probability of 30 %, hydrogen atoms are neglected for the sake of clarity. Selected bond lengths (pm): Mg1-N1 198.6(3), Mg1-N2 199.6(3), Mg1-O1 204.8(2), N1-Si1 171.4(3), N1-Si2 172.1(3), N2-Si3 170.6(3), N2-Si4 171.1(3), Mg1···Si1 325.87(13), Mg1···Si2 312.26(13), Mg1···Si3 312.50(13); bond angles (deg.): N1-Mg1-N2 130.47(11), N1-Mg1-O1 115.54(10), N2-Mg1-O1 113.98(10), Mg1-N1-Si1 123.34(15), Mg1-N1-Si2 114.60(14), Si1-N1-Si2 120.97(15), Mg1-N2-Si3 114.97(14), Mg1-N2-Si4 123.95(15), Si3-N2-Si4 120.80(14).

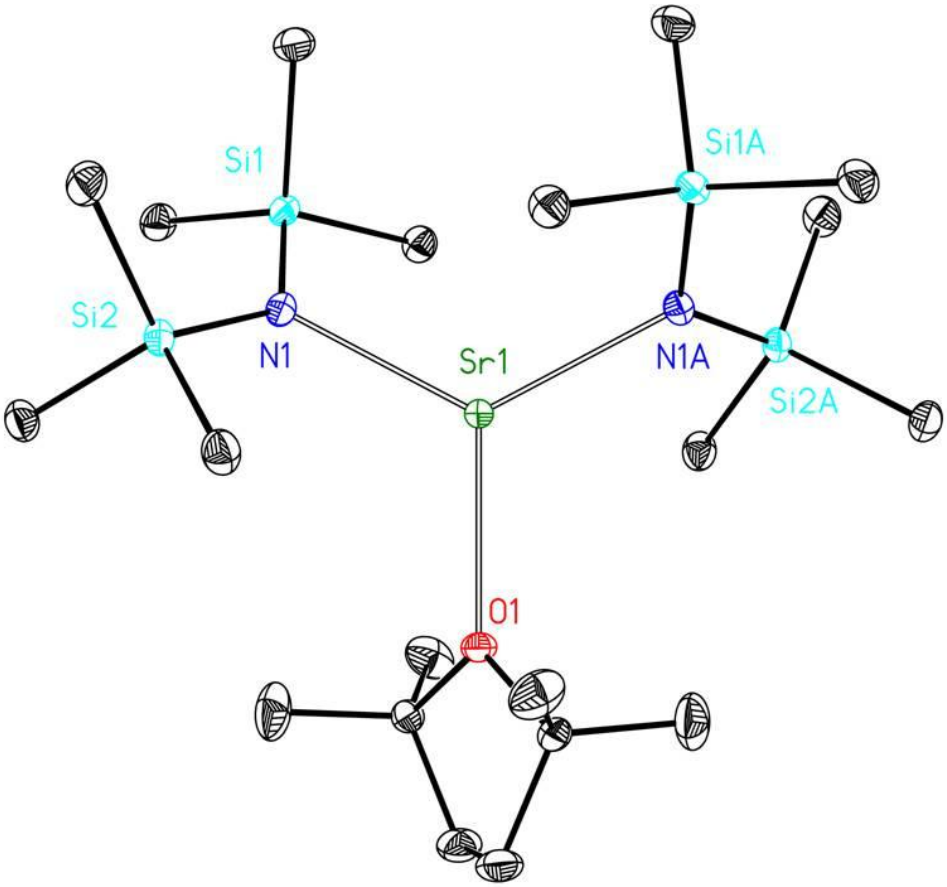

Figure S22: Molecular structure and numbering scheme of [(Me_4thf)Sr{N($SiMe_3$)$_2$}$_2$] (**3**). The ellipsoids represent a probability of 30 %, hydrogen atoms are omitted for clarity reasons. Symmetry-related atoms (-x+1, y, -z+1.5) are marked with the letter "A". Selected bond lengths (pm): Sr1-N1 240.90(13), Sr1-O1 249.61(14), N1-Si1 168.43(14), N1-Si2 168.97(14), Sr1···Si1 344.33(6), Sr1···Si2 353.23(7); bond angles (deg.): N1-Sr1-N1A 124.43(6), N1-Sr1-O1 117.79(3), Si1-N1-Si2 128.40(8), Sr1-N1-Si1 113.35(7), Sr1-N1-Si2 117.98(7).